An Algorithm for Image Segmentation in HSI Color Space

Atanaska Bosakova-Ardenska[1*], Hristina Andreeva[1], Stoicho Stoichev[2]

[1] Computer Systems and Technologies, University of Food Technologies, Plovdiv, Bulgaria

[2] Computer Systems, Technical University, Sofia, Bulgaria

Abstract: This paper presents a new segmentation algorithm that uses priority components in HSI (Hue, Saturation, Intensity) color space. The algorithm (named SegPC) is designed for HSI color space to support image understanding in different areas of human activities because this color space is modeled to be closer to humans' color perception. The innovative idea for the usage of all color components with respect to their importance is exploited in algorithm development. Two parameters are used for controlling the segmentation process, the first parameter is the number of colors used in the segmentation process and the second is the order of applying calculated thresholds for color components. The main goal of the research is the analysis of the proposed new segmentation algorithm. A set of images with different types of histograms is used for practical examination of the developed algorithm. The peak signal-to-noise ratio (PSNR) is used as a measure of the effect of image segmentation. The highest PSNR values ($\approx$22 for images with histogram near to bi-modal type and $\approx$23 for images with histogram with several peak values) are calculated for the priority of color components in which the first analyzed component is color intensity and the number of colors in the segmented image is a quarter of the number of colors in the input image. This result could be explained by the meaning of the intensity component which describes the brightness of the color and because of this, it carries a significant part of color information. The time complexity of SegPC is evaluated through theoretical analysis and experimentally. It is observed that performance time depends on three variables: first, the size of the image strongly influences time complexity (when the size of the image increases then the time for processing increases too), second, the number of colors also is related to time for processing, and third, the selected color components chosen as per the priority has a weak influence on time complexity because it defines the number of pixels which have to be additionally analyzed. The developed algorithm presents promising results. Thus, it could be applied in image analysis and natural sciences.

Keywords: image processing, segmentation, HSI color space, peak signal-to-noise ratio.

恒指色彩空间中的一种图像分割算法

　　摘要：本文提出了一种新的分割算法，该算法使用恒指（色相、饱和度、强度）颜色空间中的优先级分量。该算法（名为隔离个人电脑）专为恒指颜色空间而设计，以支持人类活动不同领域的图像理解，因为该颜色空间被建模为更接近人类的颜色感知。在算法开发中利用了使用所有颜色分量的重要性的创新理念。两个参数用于控制分割过程，第一个参数是分割过程中使用的颜色数量，第二个参数是应用计算的颜色分量阈值的顺序。研究的主要目标是分析所提出的新分割算法。一组具有不同类型直方图的图像用于对所开发算法的实际检查。峰值信噪比(信噪比)用作衡量图像分割效果的指标。计算最高信噪比值（直方图接近双峰类型的图像约为 22，直方图具有多个峰值的图像约为 23）计算颜色分量的优先级，其中第一个分析分量是颜色强度和数量分割图像中的颜色是输入图像中颜色数量的四分之一。这个结果可以用描述颜色亮度的强度分量的含义来解释，正因为如此，它携带了很大一部分颜色信息。通过理论分析和实验评估隔离个人电脑的时间复杂度。据观察，性能时间取决于三个变量：首先，图像的大小对时间复杂度有很大影响（当图像大小增加时，处理时间也会增加），

Bosakova-Ardenska et al. An Algorithm for Image Segmentation in HSI Color Space, Vol. 49 No. 6 June 2022

63

其次，颜色的数量也与时间有关第三，根据优先级选择的所选颜色分量对时间复杂度的影响很小，因为它定义了必须额外分析的像素数量。所开发的算法呈现出有希望的结果。因此，它可以应用于图像分析和自然科学。

关键词：图像处理、分割、恒指颜色空间、峰值信噪比。

1. Introduction

Image segmentation is an important step in image analysis. It is a technique of dividing a digital image into different sets of pixels, i.e., pixels in a region are similar according to some homogeneity criteria such as color, intensity, or texture, to locate and identify objects and boundaries in an image [1]. It is used for filtering noisy images, medical applications, locating objects in images, face recognition, and fingerprint recognition [2]. There are many segmentation methods, and the choice of an appropriate technique is decided by the particular image type and the problem's characteristics that have been considered [3]. The most popular techniques are for global gray-level thresholding, and many algorithms have been proposed in this direction, like the works of Rosin [4]. A different approach for image thresholding is dividing the image into more levels than objects and background. It uses multi-level thresholding, but the main problem is its large time complexity [5].

In image processing, color image segmentation is a priority task by image analysis. Researchers use algorithms for color image segmentation like mean-shift clustering [6], Markov random field models [7], and hybrid methods [8]. In addition, the statistical information for the distribution of colors of pixels (histograms) in RGB color space is used to solve the multi-level thresholding problem [9].

2. Algorithms for Image Segmentation in HSI Color Space

Image segmentation could be applied in RGB and other color spaces. Some researchers compare the results of segmentation in RGB and HSI color spaces in processing images of blood samples from patients with acute leukemia. The proposed algorithm segments each leukemia image into two regions: blast cells and background. There are applied segmentation algorithms in both color spaces to select the best technique for detecting the blast in blood sample images. The results show that using RGB color space is inappropriate in this case. On the other hand, an HSI color system and a saturation component can provide almost similar pixel values and shapes of original blasts [10].

Malaria parasites could be detected by segmenting images of red blood cells infected with malaria. It uses k-means clustering segmentation to segment the infected cell from the background. Different color components of RGB, HSI, and C-Y color models have been analyzed to identify the color component that could give significant segmentation performance. The research proved that segmentation using the S component of HSI color space is the best for obtaining fully segmented infected cells [11].

Another area where segmentation methods could be applied is raisin detection for various lighting conditions. The aim is to distinguish the observed objects into desired, undesired, and background regions. The input images are converted to HSI color space and segmented using a permutation-coded genetic algorithm. The results show that the proposed approach is effective [12].

Lesquerella canopies are used as an oil substitute in manufacturing many industrial products. They are yellow flowers that have two seasons of growth. A method for remote monitoring of flowering of *Lesquerella canopies* has been proposed. Digital cameras collect images, converted into an HSI color system to be segmented. The presented results prove that the proposed method for segmentation in the HSI color space is suitable for the purpose and not affected by variable outdoor lighting conditions [13].

It could be summarized that extracting information from some components of HSI color space has a practical application in various natural sciences. Depending on the particular characteristics of the processed images, a special processing algorithm is designed. In this context, developing automatic methods for image analysis in HSI color space based on segmentation techniques is an actual problem.

The main idea behind this research is to propose an image segmentation algorithm that deals with all color components in HSI color space using the priority of color components to extract more important information from the image.

3. Algorithm for Segmentation Using Priority Components (SegPC) in HSI Color Space

The color image is stored in digital form as a file in BMP format and described in the RGB color system. Because of this, as a preliminary step, the image has to be converted into HSI color space. The conversion is based on well know classic formulae [1]:

$$H = cos^{-1}\left\{\frac{0.5[(R-G)+(R-B)]}{[(R-G)^2+(R-B)(G-B)]^{0.5}}\right\} \qquad (1)$$

$$S = 1 - \frac{3}{R+G+B}[\min(R, G, B)] \qquad (2)$$

$$I = \frac{R+G+B}{3} \qquad (3)$$

The image presentation in HSI color space defines the sets of pixels (segments) that have to be in the same color.

3.1. Segmentation with Priority Components

Let the image be sized mxn (Im). The number of colors in segmented image k is limited to a quarter of the number of colors in the input image. Its maximum value is 64 (the intensity of color in the grayscale image is between 0 and 255). This limitation is motivated by the basic concept of segmentation - it has to reduce the number of colors to prepare images for object extraction.

Depending on priority order, the sets of pixels with different colors are defined (D_1, D_2, …, D_k). The set of pixels D_1 contains pixels colored in black by image segmentation, and the set of pixels D_k contains pixels colored in white. The other sets (D_2, D_3, …, D_{k-1}) contain pixels that have to be colored in gray with different intensities. Pixels falling in the set D_1 are the union of a part of pixels falling in A_1, a part of pixels falling in B_1, and all pixels falling in C_1. The sets of pixels A_i (i = 1, 2, …, k) are defined using the first color component in priority order (Formula 4).

$$C_{HSI}^1 \stackrel{\text{def}}{=} A_1 \cup A_2 \cup A_3 \cup ... \cup A_k = \bigcup_1^k A_i \qquad (4)$$

Every pixel belongs to only one set of pixels A_i (Formula 5).

$$A_1 \cap A_2 \cap A_3 \cap ... \cap A_k = \emptyset \qquad (5)$$

The union of sets of pixels A_i defines the image unambiguously. The sets of pixels B_i (i = 1, 2, …, k) are defined using the second color component in the priority order (formula 6), and their union defines the set A_1.

$$C_{HSI}^2 \stackrel{\text{def}}{=} B_1 \cup B_2 \cup B_3 \cup ... \cup B_k = \bigcup_1^k B_i = A_1 \qquad (6)$$

The intersection of all sets of pixels B_i is an empty set (formula 7).

$$B_1 \cap B_2 \cap B_3 \cap ... \cap B_k = \emptyset \qquad (7)$$

The sets of pixels C_i (i=1, 2, …, k) are defined using the third color component in the priority order (Formula 8), and their union defines the set B_1.

$$C_{HSI}^3 \stackrel{\text{def}}{=} C_1 \cup C_2 \cup C_3 \cup ... \cup C_k = \bigcup_1^k C_i = B_1 \qquad (8)$$

The intersection of all sets of pixels C_i is an empty set.

$$C_1 \cap C_2 \cap C_3 \cap ... \cap C_k = \emptyset \qquad (9)$$

Finally, the set of pixels D_1 could be defined by the next equation:

$$D_1 = \bigcup_2^k B_i \cup \bigcup_1^k C_i \qquad (10)$$

The second and third color components are applied to separate pixels that fall in set A_1 (colored in black) because there are presented pixels with dark color, which could contain shadows. Thus, they have to be differentiated from other pixels.

The decision to distribute pixels into defined sets of pixels (D_i; i = 1, 2, …, k) is based on two predicates. The first predicate (Formula 11) is designed to identify all pixels that must be colored in black (distributed into set D_1). The second predicate (Formula 12) implements the distribution of remaining pixels (m*n - $|D_1|$; m- width of the image, n- high of image) into sets of pixels.

D_i (i= 2, 3, …, k).

$$P(C_{HSI}^1, K_1) = \begin{cases} true\ if(Im(i,j) \le C_{HSI}^1(T_1)) \wedge (Im(i,j) \le C_{HSI}^2(T_1)) \wedge \\ \quad (Im(i,j) \le C_{HSI}^3(T_1)) \\ \quad false, otherwise \end{cases} \qquad (11)$$

The value K_1 is the black color in the segmented image, and T_1 is the first threshold value defined for the color component.

$$P(C_{HSI}^p, K_l) = \begin{cases} true\ if(Im(i,j) > C_{HSI}^p(K_l)) \\ \quad false, otherwise \end{cases} \qquad (12)$$

The p has a value of 2 or 3 and presents the second and third priority components. K_l (l= 2, 3, …, k) is a color in segmented image.

The threshold values (T_i; i= 1, 2, …, k-1) are defined as medians in a set of pixel values for every color component.

Statement 1: The distance between two couples of threshold values (T_i, T_{i+1}) and (T_j, T_{j+1}) is a constant.

Proof: Let a set S_1 be composed of all pixels which have a color value smaller than T_1 ($s_i < T_i$; i=1, 2, … (m*n/k)) and a set S_2 be composed of all pixels which have a color value smaller than T_2. The median values are defined for the sorted row of pixels (their colors) → T_1 is smaller than T_2 ($T_1 < T_2$), and all elements of S_1 are smaller than elements that fall in S_2. All elements smaller than T_2 define a set for which T_1 is a median → $|A_1| \equiv |A_2|$. Let a set S_3 be composed of all pixels with color values smaller than T_3. All elements smaller than T_3 define the set S_3. The value T_3 is also median → $|A_2| \equiv |A_3|$. With mathematical induction, it could be supposed that $|A_i| \equiv |A_{i+1}|$ => the distance between two couples of threshold values, (T_i, T_{i+1}) and (T_j, T_{j+1}), is a constant.

3.2. Region Definition

The segmented image consists of regions (segments) which are the results of the segmentation procedure. In common, the number of regions is bigger than the number of colors (K). Two regions are neighbors if their color is different; consequently, the regions with the same color are not neighbors. Let R_i and R_j be the regions with the same color.

R_i = { p_1, p_2, p_3, …, p_r }

R_j = { p_1, p_2, p_3, …, p_q }, r = q or r ≠ q

Every pixel which is part of R_i or R_j has the original color between thresholds (T_l, T_{l+1}) => one of the predicates (11 or 12) is true. The maximum distance between $\bar{p_l}$ and $\bar{p_j}$ is $|T_1 - T_{l+1}|$, and the minimum distance is zero. The variance between mathematical expectations for two regions with the same color is ε (Formula 13).

$$\left| \bar{p_i} - \bar{p_j} \right| < \varepsilon \qquad (13)$$

Let two regions, R_x and R_y, have the same color, but it is different from the color of regions R_i and R_j. The mathematical expectations for these regions (R_x and R_y) are $\overline{p_x}$ and $\overline{p_y}$. Let the pixels which are part of R_x or R_y have an original color between thresholds (T_{l+1}, T_{l+2}) => one of the predicates (11 or 12) is true. Then, the variance between R_i and R_j is smaller than between R_x and R_y.

$$\left| \overline{p_i} - \overline{p_j} \right| < \left| \overline{p_x} - \overline{p_y} \right| \tag{14}$$

Thus, the probability ($\bar{R}$) for a fixed couple of regions of Im is not more than δ ($0 \leq \delta \leq 1$).

3.3. Time Complexity

The conversion of Im into an HSI color space forms the first part of the time complexity function. This processing involves a sequence of arithmetic calculations for every pixel, and thus its complexity is N^2 (N- size of input image (m*n)). The next step of the SegPC algorithm is the calculation of thresholds, which are needed for the segmentation process as they are part of segmentation predicates. The time complexity of this calculation is NlogN, because the quick sort algorithm is used for sorting to identify median values. The predicates of time complexity depend on two parameters, namely, the number of colors (K) and number of pixels that form the set A_1.

$$t_{predicates} = f(K, |A_1|) \tag{15}$$

When the number of colors increases, the time for processing also increases. Some fluctuations may appear in this trend because the number of pixels that fall in set A_1 also influences the time for processing.

$$T = N^2 + NlogN + t_{predicates} \tag{16}$$

The upper asymptotic bound of the time complexity of SegPC is O (N^2).

4. Peak Signal-to-Noise Ratio and Its Application

Peak signal-to-noise ratio (PSNR) is used to calculate the ratio between the maximum possible signal power and the power of the distortion noise that affects the quality of the representation. This ratio is usually calculated as a logarithmic quantity using the decibel scale. PSNR is described mathematically by Equations (17) and (18).

$$PSNR = 10 \log_{10}\left(\frac{MAX_I^2}{MSE}\right) \tag{17}$$

$$MSE = \frac{1}{mn}\sum_{i=0}^{m-1}\sum_{j=0}^{n-1}[I(i,j) - K(i,j)]^2 \tag{18}$$

where *MAX* is the highest possible value of the signal. If the input is a grayscale image of 8 bits, then *MAX* = 255. *MSE* is the mean squared error between the original image and the reconstructed image. The parameters *m* and *n* are the number of rows and columns, respectively, in the image. The PSNR is inversely proportional to the MSE [14].

4.1. Usage in Filtering

PSNR is often used to evaluate denoising algorithms. Mohideen et al. [15] discussed a method for additive random noise that can easily be removed using simple threshold methods. Wavelet denoising scheme thresholds the wavelet coefficients arising from the standard discrete wavelet transform. Research has been proposed on the suitability of different wavelet bases and the size of different neighborhoods on the performance of image denoising algorithms in terms of PSNR [15].

Erkan et al. proposed a method to remove salt and pepper noise and used PSNR to compare the obtained results with the results of other methods [16].

Sara et al. performed simulation experiments using Gaussian noise through a Gaussian filtering technique. The image quality was evaluated by applying different metrics, such as structured similarity indexing method (SSIM), feature similarity indexing method (FSIM), MSE, and PSNR. The results were similar for all used metrics. If the noise level is increasing, then the recovery quality of the output image will decrease [17].

Image denoising is an important part of the analysis of MRI brain scan images because it removes the undesirable noisy components. Denoising technique plays a significant role in sustaining the stability between two components: noise removal and preservation of image features. Different methods for denoising are applied on a dataset of MRI images, and the results are validated by calculating the PSNR value [18].

4.2. Evaluation of Segmentation

PSNR is also used to measure contrast enhancement. This ratio is used as a quality measurement between original and contrast-enhanced images. The most appropriate image processing method can be selected by comparing the results obtained for the PSNR [19].

Jumb et al. presented an approach for color image segmentation. The proposed processing includes the conversion of images to an HSV color space and segmentation based on Otsu's method and K-means clustering for regions merging. The segmented images obtained through processing with the proposed approach and other algorithms are compared using the PSNR value [20].

Other researchers also used image segmentation techniques based on the kernel subtractive and k-means clustering algorithm. Their results are compared with the segmentation results using the PSNR value in order to validate the effectiveness of the proposed method [21].

Wang et al. [22] proposed an automatic segmentation system to separate maize leaves from a complex background in digital images under different light conditions. The obtained results are compared with the results of processing with other segmentation algorithms. The PSNR value is calculated to measure how close the segmentation image is to the standard

image and how it affects the illumination changes [22].

Image segmentation methods are also applied in medical imaging systems, for example, to analyze lung images [25]. Three methods are used for image segmentation: connected threshold, neighborhood connected, and threshold level set segmentation. The different methods are compared based on the calculated performance evaluation parameters MSE and PSNR [23].

Bao et al. [24] proposed a hybrid algorithm for color image segmentation. Otsu's method and Kapur's entropy are used to determine the segmentation threshold values. The proposed a hybrid algorithm uses Harris hawks optimization and differential evolution. Seven known algorithms are compared using a set of images. Some measures, including PSNR, are used to evaluate the performance of each algorithm [24].

In the present paper, PSNR is used to evaluate the proposed algorithm. According to the obtained results, the most appropriate number of colors and the priority of components in image segmentation are set.

5. Experimental Results

A set of eight images is used to test the proposed algorithm. The images have different sizes as follows: WCB structure (3385×3393), CST laboratory (3500×2625), Grebna Baza (1920×1440), ice cream (3500×2333), Lena (512×512), cheese samples (2560×1440), peppers (512×512), and tulips (1024×768). Two of the test images (Lena and peppers) are popular

in image processing [1], and the remaining six images are captured in laboratories of the University of Food Technologies (which captures the structure of different types of food) in the city of Plovdiv. The histograms of the test images are presented on Fig. 1.

Each of these images is converted to grayscale using the proposed segmentation algorithm. Before the segmentation is started, the desired number of colors and the priority of the components are set. The algorithm is tested with 2, 4, 6, 8, 10, 20, 30, 40 colors, and a quarter of the maximum possible colors of the image. The test images present different objects captured in different lighting conditions, so different maximum numbers of colors are obtained. For the image "WCB structure," the maximum number of colors is 52, whereas for "CST Laboratory," "Grebna Baza," and "cheese samples," 63 colors are used. The "ice cream" colors are 61 and 55 for "Lena." For "peppers" and "tulips," 57 and 62 colors are used, respectively. The segmented images are saved in BMP format.

The results for four images with different histogram types are presented in Fig. 2. The image "WCB structure" presents the structure of Bulgarian white cheese in brine, the image "Grebna Baza" is captured on a rowing channel in Plovdiv, and the image "Lena" and "peppers" are well known in the field of image processing. It used color components' priority 0 ($I^1 S^2 H^3$) and selected some colors for segmentation.
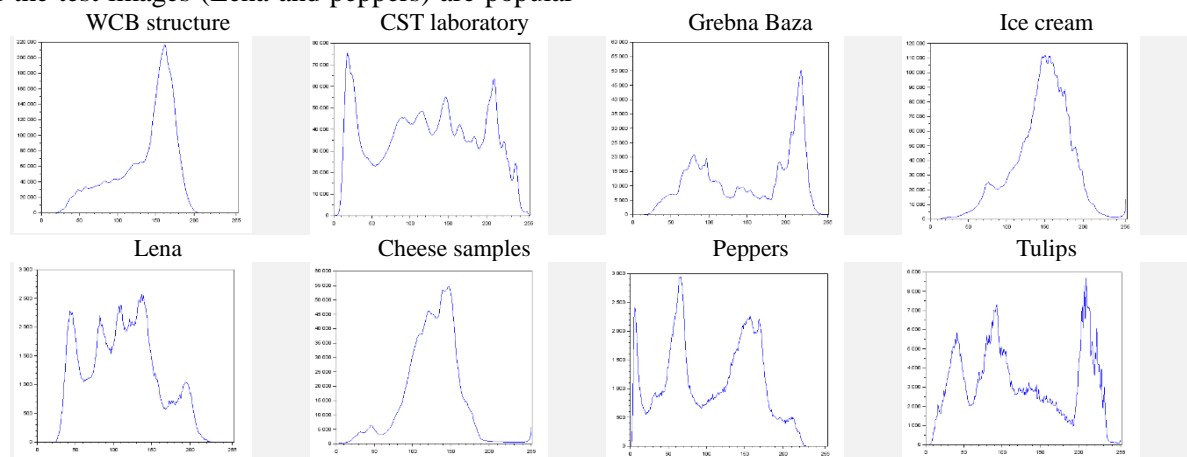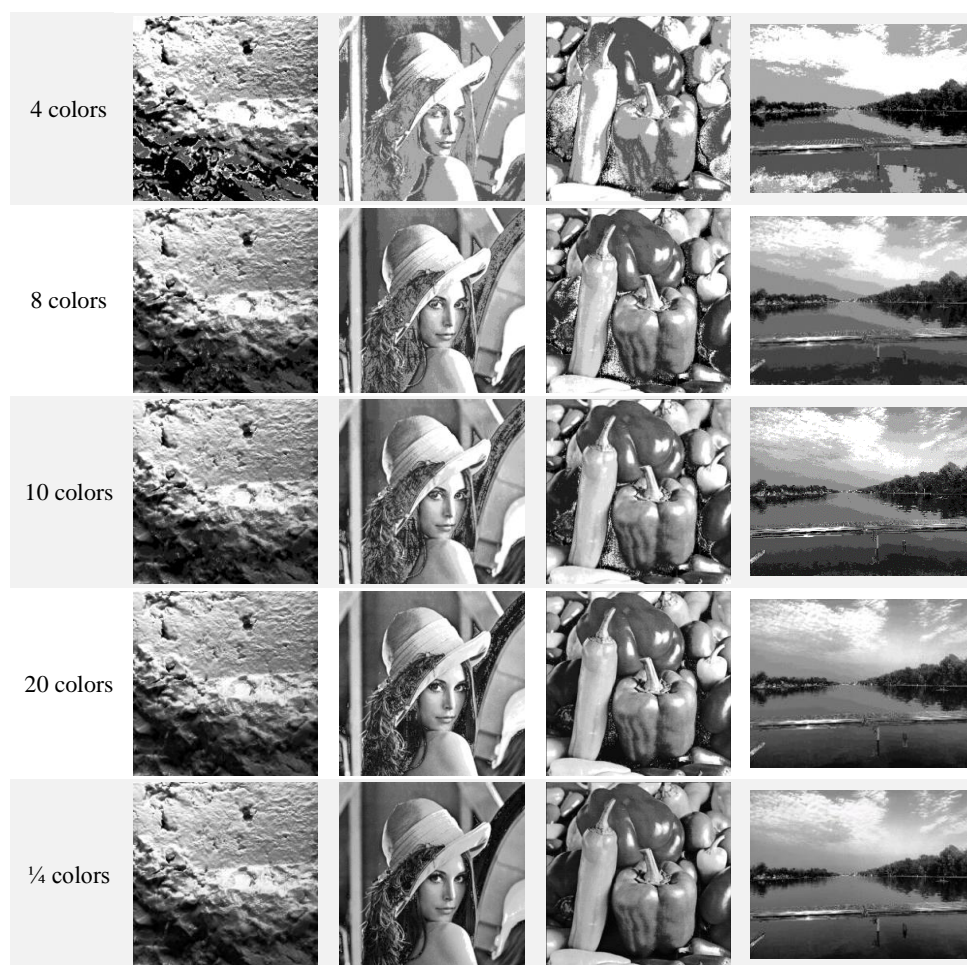

Fig. 1 Image histograms

Bosakova-Ardenska et al. An Algorithm for Image Segmentation in HSI Color Space, Vol. 49 No. 6 June 2022

67

Fig. 2 Results for color components' priority 0 ($I^1S^2H^3$)

The obtained results for images "Lena" and "peppers" are presented in Fig. 3 and 4, using all possible color types, components priority, and four versions of color number. It is observed that processing results for image "Lena" are quite different in different segmentation modes (with different order of priority components), especially when the number of colors is higher than two. This image has a histogram with many small peaks (Fig. 1) and a high contrast among areas with different color intensities (hue). The presence of pixels with colors in different gamma (near to different basic colors like red and blue) significantly influences segmentation results in these modes, which are used as a first priority component Hue. The segmented images of "peppers" are very similar when only two colors are used in all possible modes to prioritize color components. The "peppers" image has three main peaks in a histogram. The segmentation with 20 and more colors with intensity usage as a first priority component leads to good quality results.
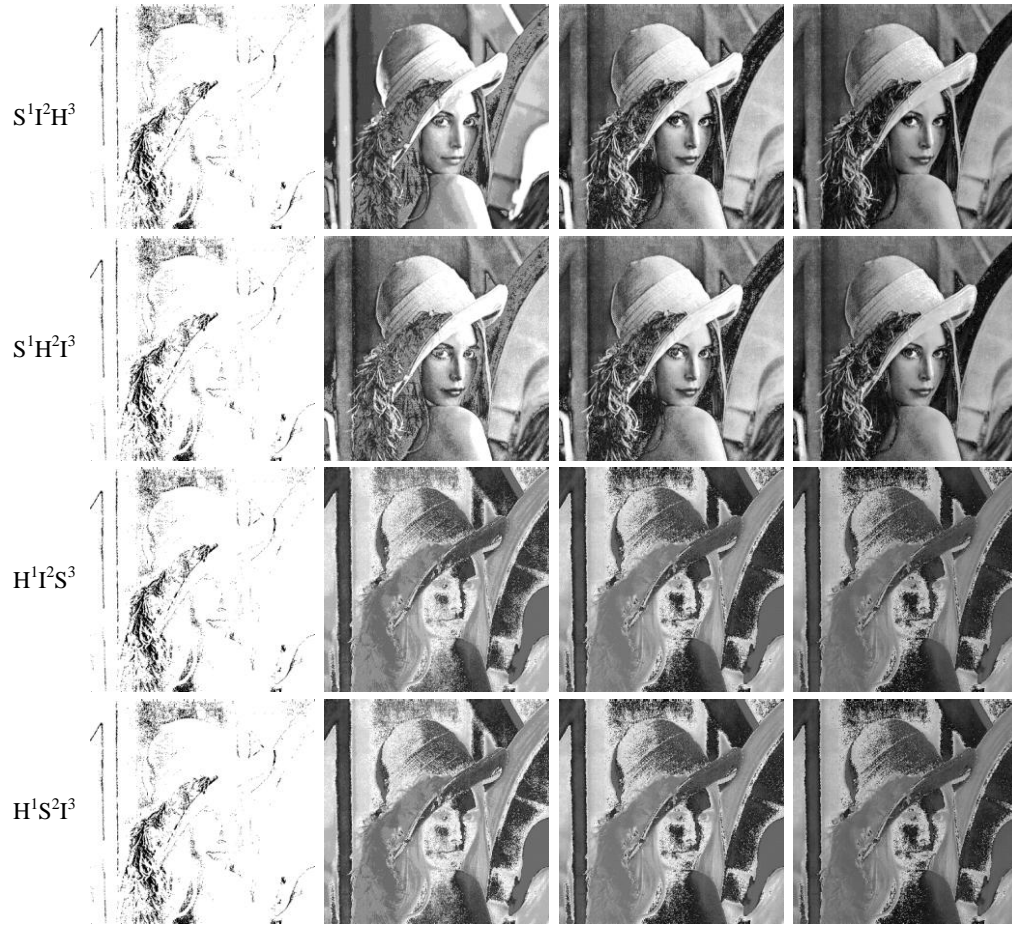
$S^1I^2H^3$

$S^1H^2I^3$

$H^1I^2S^3$

$H^1S^2I^3$

Fig. 3 Results for image "Lena" with all components' priority

| 2 colors | 8 colors | 20 colors | ¼ colors |

$I^1S^2H^3$

$I^1H^2S^3$

$S^1I^2H^3$

$S^1H^2I^3$

69

Bosakova-Ardenska et al. An Algorithm for Image Segmentation in HSI Color Space, Vol. 49 No. 6 June 2022
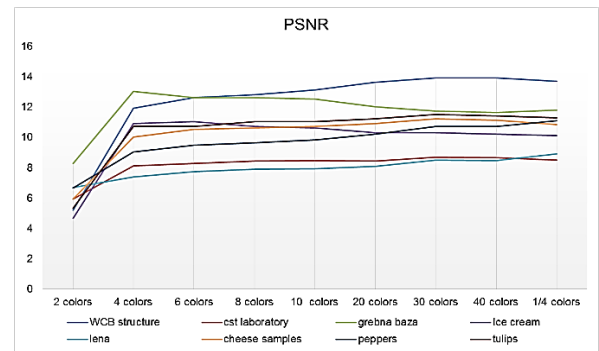
$H^1I^2S^3$

$H^1S^2I^3$

Fig. 4 Results for image "peppers" with all components' priority

5.1. PSNR

A program has been created in Scilab to calculate the PSNR value using formulae 17 and 18. The images segmented with the proposed algorithm (SegPC) are compared with the original image. For each image, 54 PSNR values (6 modes [orders of priority components] x 9 values for the number of colors) are calculated. The PSNR values for couples of priority modes with the same first color component (for example, priority 0 and priority 1 have first priority color component Intensity) are very similar because the set of pixels A1 in these modes is the same. Fig. 5-7 show the PSNR values for priorities 0, 2, and 4, respectively. It is observed that the highest PSNR values are measured for priority 0 (first processed component is intensity, second is saturation, and third is hue). This observation could be explained by the nature of the intensity component. Which implements the brightness of the color, and because of this, it significantly forms the sense of color.

In all discussed priority modes, the lowest PSNR value is calculated for binary image (two colors). A significant increase in PSNR value is measured for the image with four colors compared to the same image segmented with two colors. PSNR value increases when the number of colors increases. In Priority Mode 4 (Fig. 7), the lowest PSNR values are calculated for image "Lena," which corresponds with the visual evaluation of segmented images (Fig. 3, mode $H^1I^2S^3$).
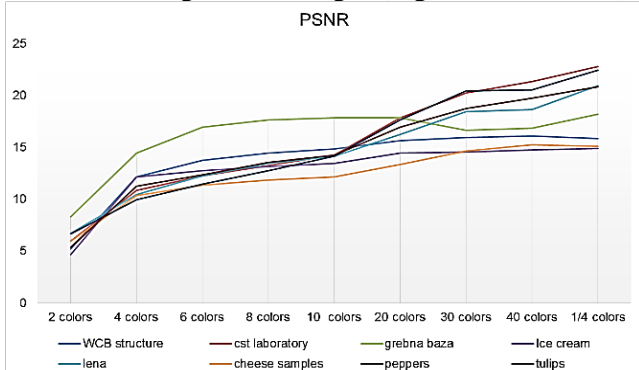
Fig. 5 PSNR for Priority 0 ($I^1S^2H^3$)
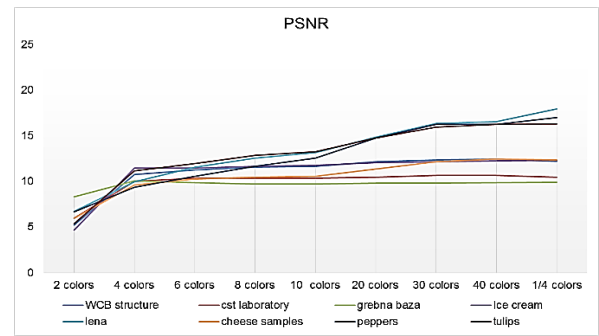
Fig. 6 PSNR for Priority 2 ($S^1I^2H^3$)

Fig. 7 PSNR for Priority 4 ($H^1I^2S^3$)

5.2. Performance Evaluation

The experimental time complexity evaluation is performed in the same conditions, as follows:

1) Every image is processed ten times with selected parameters (priority of color components, number of colors).

2) The measured time (ms) is summarized as an average value, and a standard deviation is calculated too.

3) It uses a mobile computer system ASUS ROG-STRIX with processor Intel(R) Core(TM) i5-10300H CPU @ 2.50GHz, 16MB memory, and Windows 10 (64 bits) operating system.

Fig. 8 presents the total time for image segmentation using 2, 10, and 20 colors and the priority of color components Intensity->Saturation->Hue ($I^1S^2H^3$).

Increasing the number of pixels (the size of the image is shown on the x-axis) leads to increased

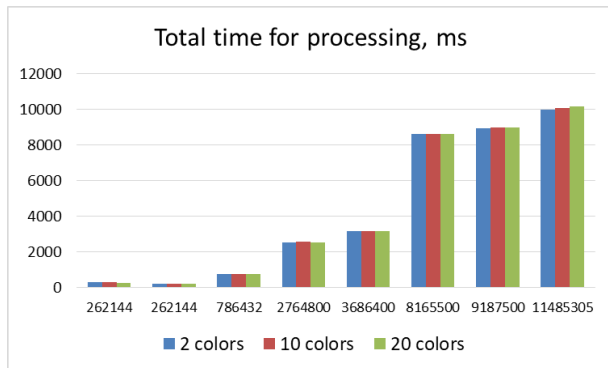processing time. The trend of the presented function is quadratic.

Fig. 8 Average time for processing of all images

Tables 1 and 2 present standard deviations (σ) calculated for the time of processing two tested images. It is observed that the standard deviation in the measured time is higher for the bigger image, which could be explained by the higher value of the measured times when the bigger image is processed. For all test images, the standard deviation of performance time, calculated as a percent of measured time, is between 0.5% and 17% (the average value is about 4.9%). The average standard deviation ($\bar{\sigma}$) for all test images is about 8.3.

Table 1 Standard deviation (σ) of measured time for segmentation of small image (lena.bmp)

	2	4	6	8	10	20	40	¼ colors
$I^1S^2H^3$	2.24	1.94	1.18	1.42	1.20	1.66	0.92	1.54
$I^1H^2S^3$	0.66	1.36	1.04	1.60	2.53	0.54	1.17	1.55
$S^1I^2H^3$	0.46	1.41	1.42	1.64	1.47	2.06	0.46	1.81
$S^1H^2I^3$	0.98	1.89	1.28	1.49	1.19	0.60	1.00	1.50
$H^1I^2S^3$	1.30	1.69	1.20	1.81	1.40	2.05	1.14	0.54
$H^1S^2I^3$	0.66	1.69	1.55	1.17	1.30	0.64	1.73	1.76

Table 2 Standard deviation (σ) of measured time for segmentation of big image (WCB structure.bmp)

	2	4	6	8	10	20	40	¼ colors
$I^1S^2H^3$	17.67	28.84	21.58	12.10	25.20	18.61	26.99	12.28
$I^1H^2S^3$	11.58	12.94	11.55	15.21	18.65	7.51	11.46	15.60
$S^1I^2H^3$	20.77	57.81	21.76	24.85	9.90	15.57	6.64	19.08
$S^1H^2I^3$	16.07	20.61	3.10	8.91	5.19	9.16	17.81	5.60
$H^1I^2S^3$	18.24	33.43	14.17	5.66	11.12	9.86	24.80	43.32
$H^1S^2I^3$	23.55	37.47	23.40	31.04	21.58	11.40	10.10	8.52

The variance in measured time values is typical for performance on modern computer systems because they work in multitasking mode, and the loading of a system depends on various factors (such as the execution of background programs that check for updates).

Fig. 9-12 present the average time for segmentation ($t_{predicates}$) of four images using six modes for priority of color components and eight different values for several colors.

The notations "Priority 0" to "Priority 5" corresponds with the priorities of color components as follows:

"Priority 0" ≡ $I^1S^2H^3$; "Priority 1" ≡ $I^1H^2S^3$;
"Priority 2" ≡ $S^1I^2H^3$; "Priority 3" ≡ $S^1H^2I^3$;
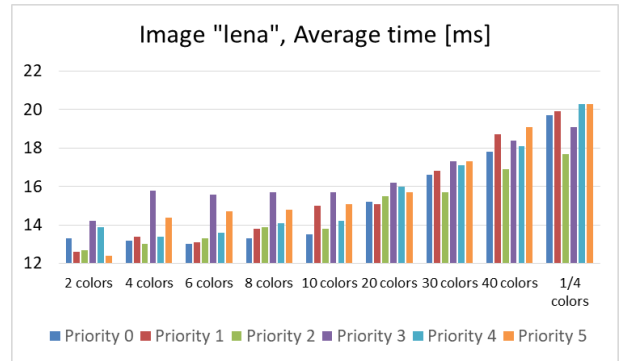"Priority 4" ≡ $H^1I^2S^3$; "Priority 5" ≡ $H^1S^2I^3$.

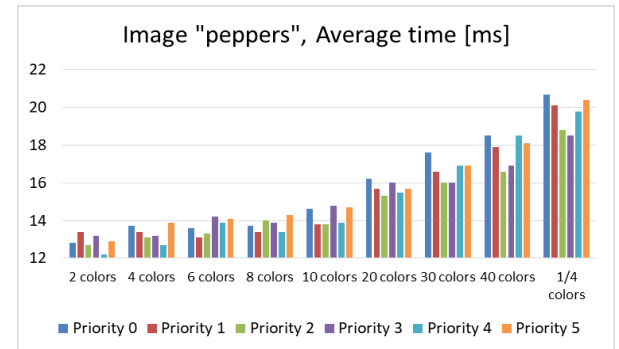Fig. 9 Average time for segmentation for image "Lena"

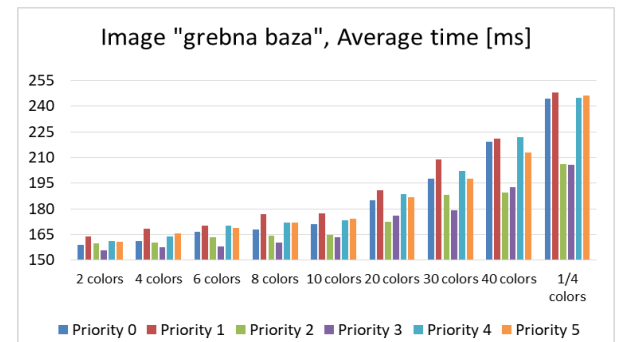Fig. 10 Average time for segmentation for image "Peppers"

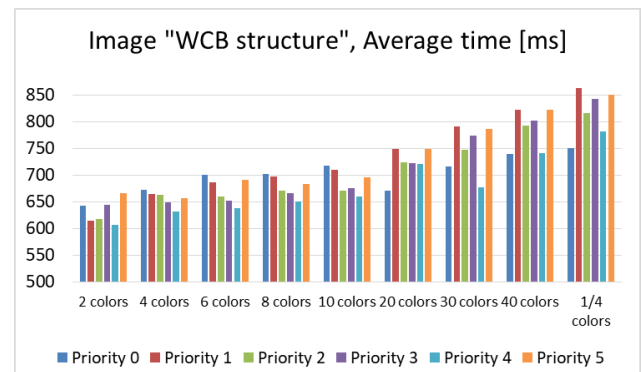Fig. 11 Average time for segmentation for image "Grebna Baza"

Fig. 12 Average time for segmentation for image "WCB structure"

It is observed that, when the number of colors is a constant, then the segmentation mode ("Priority 0" to "Priority 5") influences the time for segmentation. The differences in measured values for segmentation time are bigger when the number of colors is higher. In some cases, the time for segmentation decreases when the number of colors increases. For example, the average time for segmentation of image "WCB structure" for ten colors is 718.1 ms, but, for 20 colors,

Bosakova-Ardenska et al. An Algorithm for Image Segmentation in HSI Color Space, Vol. 49 No. 6 June 2022

71

it is 670.6 ms. This effect could be explained by a big number of pixels falling in set A_1 at a small number of colors and a significant decrease in their number when the number of colors increases (the pixels falling in set A_1 are processed with predicates using the second and third color components, which involves more calculations).

In summary, in more cases, the time for segmentation increases when the number of colors increases.

6. Conclusion

This paper discusses a new image segmentation algorithm (SegPC – segmentation with priority components) that processes the images in HSI color space. The algorithm uses region definition based on the selected priority order of color components. The usage of all color components of HSI color space together is a novelty in the field of image segmentation. The data selected as a first priority component have a primary meaning, but the other two color components also contribute to the segmentation result. Test images are used to evaluate the performance of SegPC in two aspects:

1) The quality of segmentation is evaluated for different priority orders of color components and different numbers of colors in segmented images using PSNR as a measure;

2) The time complexity of the algorithm is explored theoretically and experimentally.

The results could be summarized as follows:

- It is preferred that the number of colors for segmentation be higher than four because, in this case, the PSNR value is high, which indicates that the segmented image keeps a significant part of the information;

- The selected mode for priority of color components influences segmentation results, so the appropriate mode has to be chosen according to the specific purpose of the processing;

- The size of input images significantly influences the time for processing, and the choice of a not very high number of colors for segmentation leads to decreased performance time.

A limitation of the proposed algorithm could be the usage of parameters for the number of colors in a segmented image. In the future, the proposed algorithm could be upgraded with some methods for automatically identifying the best number of colors for the segmentation. Another direction for future research is investigating applications of the developed algorithm in image analysis in various scientific fields such as food quality evaluation and object recognition.

References

[1] GONZALEZ R. C., & WOODS R. E. *Digital Image Processing*. 4th ed. Pearson Education Limited, New York, 2018. https://www.codecool.ir/extra/2020816204611411Digital.Image.Processing.4th.Edition.www.EBooksWorld.ir.pdf

[2] DANEV A., GABROVA R., YANEVA-MARINOVA T., and ANGELOV A. Application possibilities of open-source software for microbiological analyses. *Bulgarian Chemical Communications,* 2018, 50: 239-245. http://bcc.bas.bg/BCC_Volumes/Volume_50_Special_G_2018/50G_PD_239-245.147.pdf

[3] DASS R., PRIYANKA, and DEVI S. Image segmentation techniques. *International Journal of Electronics & Communication Technology*, 2012, 3(1): 66-70. http://www.iject.org/vol3issue1/rajeshwar.pdf

[4] ROSIN P. L. Unimodal thresholding. *Pattern Recognition*, 2001, 34(11): 2083–2096. https://doi.org/10.1016/S0031-3203(00)00136-9

[5] WANG S., CHUNG F. L., and XIONG F. A novel image thresholding method based on Parzen window estimate. *Pattern Recognition*, 2008, 41(1): 117-129. https://doi.org/10.1016/j.patcog.2007.03.029

[6] LUO Q., & KHOSHGOFTAAR T. M. Unsupervised multiscale color image segmentation based on MDL principle. *IEEE Transactions on Image Processing*, 2006, 15(9): 2755-2761. https://doi.org/10.1109/TIP.2006.877342

[7] MIGNOTTE M. A label field fusion Bayesian model and its penalized maximum rand estimator for image segmentation. *IEEE Transactions on Image Processing*, 2010, 19(6): 1610-1624. https://doi.org/10.1109/TIP.2010.2044965

[8] TAN K. S., & ISA N. A. M. Color image segmentation using histogram thresholding – Fuzzy C-means hybrid approach. *Pattern Recognition*, 2011, 44(1): 1-15. https://doi.org/10.1016/j.patcog.2010.07.013

[9] RAJINIKANTH V., & COUCEIRO M. S. RGB Histogram Based Color Image Segmentation Using Firefly Algorithm. *Procedia Computer Science*, 2015, 46: 1449-1457. https://doi.org/10.1016/j.procs.2015.02.064

[10] HARUN N. H., MASHOR M. Y., MOKHTAR N. R., AIMI SALIHAH A. N., HASSAN R., RAOF R. A. A., and OSMAN M. K. Comparison of acute leukemia Image segmentation using HSI and RGB color space. Proceedings of the 10th International Conference on Information Science, Signal Processing and their Applications, Kuala Lumpur, 2010, pp. 749-752. https://www.researchgate.net/publication/221616748

[11] ABDUL-NASIR A. S., MASHOR M. Y., and MOHAMED Z. Colour image segmentation approach for detection of malaria parasites using various colour models and k-means clustering. *WSEAS Transactions on Biology and Biomedicine*, 2013, 10(1): 41-55. https://wseas.org/multimedia/journals/biology/2013/085708-103.pdf

[12] ABBASGHOLIPOUR M., OMID M., KEYHANI A., and MOHTASEBI S. S. Color image segmentation with genetic algorithm in a raisin sorting system based on machine vision in variable conditions. *Expert Systems with Applications,* 2011, 38(4): 3671-3678. https://doi.org/10.1016/j.eswa.2010.09.023

[13] THORP K. R., & DIERIG D. A. Color image segmentation approach to monitor flowering in lesquerella. *Industrial Crops and Products*, 2011, 34(1): 1150-1159. https://doi.org/10.1016/j.indcrop.2011.04.002

[14] FARDO F. A., CONFORTO V. H., DE OLIVEIRA F. C., and RODRIGUES P. S. *A formal evaluation of PSNR as quality measurement parameter for image segmentation*

algorithms, 2016. https://arxiv.org/abs/1605.07116

[15] KOTHER MOHIDEEN S., ARUMUGA PERUMAL S., and MOHAMED SATHIK M. Image Denoising Using Discrete Wavelet Transform. *International Journal of Computer Science and Network Security*, 2008, 8(1): 213-216.

[16] ERKAN U., GÖKREM L., and ENGINOĞLU S. Different applied median filter in salt and pepper noise. *Computers & Electrical Engineering*, 2018, 70: 789-798. https://doi.org/10.1016/j.compeleceng.2018.01.019

[17] SARA U., AKTER M., and UDDIN M. S. Image quality assessment through FSIM, SSIM, MSE and PSNR—a comparative study. *Journal of Computer and Communications,* 2019, 7(3): 8-18. https://doi.org/10.4236/jcc.2019.73002

[18] ELHOSENY M., & SHANKAR K. Optimal bilateral filter and convolutional neural network based denoising method of medical image measurements. *Measurement*, 2019, 143: 125-135. https://doi.org/10.1016/j.measurement.2019.04.072

[19] BABY J., & KARUNAKARAN V. Bi-level weighted histogram equalization with adaptive gamma correction. *International Journal of Computational Engineering Research*, 2014, 4(3): 25-30. http://citeseerx.ist.psu.edu/viewdoc/download?doi=10.1.1.58 7.3454&rep=rep1&type=pdf#page=79

[20] JUMB V., SOHANI M., and SHRIVAS A. Color image segmentation using K-means clustering and Otsu's adaptive thresholding. *International Journal of Innovative Technology and Exploring Engineering*, 2014, 3(9): 72-76. https://www.ijitee.org/wp-content/uploads/papers/v3i9/I1495023914.pdf

[21] DHANACHANDRA N., & CHANU Y. J. A new approach of image segmentation method using K-means and kernel based subtractive clustering methods. *International Journal of Applied Engineering Research,* 2017, 12(20): 10458-10464. https://www.ripublication.com/ijaer17/ijaerv12n20_171.pdf

[22] WANG P., ZHANG Y., JIANG B., and HOU J. An maize leaf segmentation algorithm based on image repairing technology. *Computers and Electronics in Agriculture*, 2020, 172: 105349. https://doi.org/10.1016/j.compag.2020.105349

[23] AMANDA A. R., & WIDITA R. Comparison of image segmentation of lungs using methods: connected threshold, neighborhood connected, and threshold level set segmentation. *Journal of Physics: Conference Series,* 2016, 694(1): 012048. https://doi.org/10.1088/1742-6596/694/1/012048

[24] BAO X., JIA H., and LANG C. A Novel Hybrid Harris Hawks Optimization for Color Image Multilevel Thresholding Segmentation. *IEEE Access*, 2019, 7: 76529-76546. https://doi.org/10.1109/ACCESS.2019.2921545

[25] KELAIN M. J. Compatibility of Enhancement and Segmentation of Digital Image Processing in Medical Applications. *Journal of Southwest Jiaotong University,* 2020, 55(1). https://doi.org/10.35741/issn.0258-2724.55.1.50

参考文:

[1] GONZALEZ R. C. 和 WOODS R. E. 数字图像处理。第 4 版。培生教育有限公司，纽约，2018 年。https://www.codecool.ir/extra/2020816204611411Digital.Image.Processing.4th.Edition.www.EBooksWorld.ir.pdf

[2] DANEV A.、GABROVA R.、YANEVA-MARINOVA T. 和 ANGELOV A. 用于微生物分析的开源软件的应用可能性。保加利亚化学通讯，2018，50：239-245。http://bcc.bas.bg/BCC_Volumes/Volume_50_Special_G_20 18/50G_PD_239-245.147.pdf

[3] DASS R.、PRIYANKA 和 DEVI S. 图像分割技术。国际电子与通信技术杂志，2012，3(1)：66-70。http://www.iject.org/vol3issue1/rajeshwar.pdf

[4] ROSIN P. L. 单峰阈值。模式识别，2001，34（11）：2083-2096。https://doi.org/10.1016/S0031-3203(00)00136-9

[5] WANG S., CHUNG F. L., 和 XIONG F. 基于帕尔森窗口估计的新型图像阈值方法。模式识别，2008，41（1）：117-129。https://doi.org/10.1016/j.patcog.2007.03.029

[6] LUO Q., & KHOSHGOFTAAR T. M. 基于 MDL 原理的无监督多尺度彩色图像分割。IEEE 图像处理汇刊，2006，15(9)：2755-2761。https://doi.org/10.1109/TIP.2006.877342

[7] MIGNOTTE M. 用于图像分割的标签场融合贝叶斯模型及其惩罚最大随机数估计器。IEEE 图像处理汇刊，2010，19(6)：1610-1624。https://doi.org/10.1109/TIP.2010.2044965

[8] TAN K. S. 和 ISA N. A. M. 使用直方图阈值的彩色图像分割——模糊 C 均值混合方法。模式识别，2011，44（1）：1-15。https://doi.org/10.1016/j.patcog.2010.07.013

[9] RAJINIKANTH V., & COUCEIRO M. S. 使用萤火虫算法的基于 RGB 直方图的彩色图像分割。普罗西迪亚计算机科学，2015，46：1449-1457。https://doi.org/10.1016/j.procs.2015.02.064

[10] HARUN N.H.、MASHOR M.Y.、MOKHTAR N.R.、AIMI SALIHAH A.N.、HASSAN R.、RAOF R.A.A. 和 OSMAN M.K. 使用恒指和 RGB 颜色空间进行急性白血病图像分割的比较。第 10 届信息科学、信号处理及其应用国际会议论文集，吉隆坡，2010 年，第 749-752 页。https://www.researchgate.net/publication/221616748

[11] ABDUL-NASIR A. S. 、 MASHOR M. Y. 和 MOHAMED Z. 使用各种颜色模型和 k-均值聚类检测疟原虫的彩色图像分割方法。WSEAS 生物学和生物医学汇刊，2013，10(1)：41-55。https://wseas.org/multimedia/journals/biology/2013/085708-103.pdf

[12] ABBASGHOLIPOUR M.、OMID M.、KEYHANI A. 和 MOHTASEBI S. S. 在可变条件下基于机器视觉的葡萄干分拣系统中使用遗传算法进行彩色图像分割。具有应用程序的专家系统，2011，38(4)：3671-3678。https://doi.org/10.1016/j.eswa.2010.09.023

Bosakova-Ardenska et al. An Algorithm for Image Segmentation in HSI Color Space, Vol. 49 No. 6 June 2022

73

[13] THORP K. R. 和 DIERIG D. A. 彩色图像分割方法监测莱斯克雷拉的开花情况。工业作物和产品，2011，34（1）：1150-1159。https://doi.org/10.1016/j.indcrop.2011.04.002

[14] FARDO F. A.、CONFORTO V. H.、DE OLIVEIRA F. C. 和 RODRIGUES P. S. 信噪比作为图像分割算法的质量测量参数的正式评估，2016 年。https://arxiv.org/abs/1605.07116

[15] KOTHER MOHIDEEN S.、ARUMUGA PERUMAL S. 和 MOHAMED SATHIK M. 使用离散小波变换进行图像去噪。国际计算机科学与网络安全杂志，2008，8(1): 213-216.

[16] ERKAN U.、GÖKREM L. 和 ENGINOĞLU S. 在椒盐噪声中应用不同的中值滤波器。计算机与电气工程，2018，70：789-798。https://doi.org/10.1016/j.compeleceng.2018.01.019

[17] SARA U.、AKTER M. 和 UDDIN M. S. 通过 FSIM、SSIM、MSE 和信噪比进行图像质量评估——一项比较研究。计算机与通信学报，2019，7(3): 8-18. https://doi.org/10.4236/jcc.2019.73002

[18] ELHOSENY M.、& SHANKAR K. 基于最优双边滤波器和卷积神经网络的医学图像测量去噪方法。测量，2019，143：125-135。https://doi.org/10.1016/j.measurement.2019.04.072

[19] BABY J.、& KARUNAKARAN V. 具有自适应伽马校正的双级加权直方图均衡。国际计算工程研究杂志, 2014, 4(3): 25-30. http://citeseerx.ist.psu.edu/viewdoc/download?doi=10.1.1.587.3454&rep=rep1&type=pdf#page=79

[20] JUMB V.、SOHANI M. 和 SHRIVAS A. 使用 K 均值聚类和大津自适应阈值的彩色图像分割。国际创新技术与探索工程杂志，2014, 3(9): 72-76. https://www.ijitee.org/wp-content/uploads/papers/v3i9/I1495023914.pdf

[21] DHANACHANDRA N.、& CHANU Y. J. 一种使用 K-均值和基于核的减法聚类方法的图像分割方法的新方法。国际应用工程研究杂志，2017，12(20): 10458-10464. https://www.ripublication.com/ijaer17/ijaerv12n20_171.pdf

[22] WANG P.、ZHANG Y.、JIANG B.、和 HOU J. 基于图像修复技术的玉米叶片分割算法。农业中的计算机和电子产品，2020 年，172：105349。https://doi.org/10.1016/j.compag.2020.105349

[23] AMANDA A. R. 和 WIDITA R. 使用方法比较肺图像分割：连接阈值、邻域连接和阈值水平集分割。物理学杂志：系列会议，2016，694(1)：012048。https://doi.org/10.1088/1742-6596/694/1/012048

[24] BAO X.、JIA H.、和 LANG C. 一种用于彩色图像多级阈值分割的新型混合哈里斯老鹰队优化。IEEE 访问，2019，7：76529-76546。https://doi.org/10.1109/ACCESS.2019.2921545

[25] KELAIN M. J. 医学应用中数字图像处理增强和分割的兼容性。西南交通大学学报，2020，55(1). https://doi.org/10.35741/issn.0258-2724.55.1.50